Science of the Total Environment 609 (2017) 1103–1113

Contents lists available at ScienceDirect

Science of the Total Environment

journal homepage: www.elsevier.com/locate/scitotenv

Total free radical species and oxidation equivalent in polluted air

Guoying Wang [a,*], Shiming Jia [a], Xiuli Niu [b], Haoqi Tian [a], Yanrong Liu [a], Xuefu Chen [a], Lan Li [a], Yuanhang Zhang [c,*], Gaofeng Shi [a,*]

[a] School of Petrochemical Engineering, Lanzhou University of Technology, Lanzhou, 730050, China
[b] Gansu Province Food Inspection Institute, Lanzhou 730050, China
[c] College of Environmental Sciences and Engineering, Peking University, Beijing 100871, China

HIGHLIGHTS

- Total free radicals linear dependence on ozone at higher temperature.
- Total free radicals linear delay dependence on particulate matters at lower temperature.
- Total free radical oxidation capacity roughly matches tobacco smoke.
- Chromatographic fingerprint similarity indicating effect of total free radicals in polluted air.

GRAPHICAL ABSTRACT

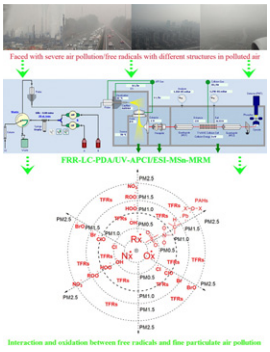

ARTICLE INFO

Article history:
Received 24 April 2017
Received in revised form 24 July 2017
Accepted 26 July 2017
Available online 4 August 2017

Editor: D. Barcelo

Keywords:
Free radicals
Human health
Linear correlation
Oxidation equivalent
Polluted air

ABSTRACT

Free radicals are the most important chemical intermediate or agent of the atmosphere and influenced by thousands of reactants. The free radicals determine the oxidizing power of the polluted air. Various gases present in smog or haze are oxidants and induce organ and cellular damage via generation of free radical species. At present, however, the high variability of total free radicals in polluted air has prevented the detection of possible trends or distributions in the concentration of those species. The total free radicals are a kind of contaminants with colorless, tasteless characteristics, and almost imperceptible by human body. Here we present total free radical detection and distribution characteristics, and analyze the effects of total free radicals in polluted air on human health. We find that the total free radical values can be described by not only a linear dependence on ozone at higher temperature period, but also a linear delay dependence on particulate matter at lower temperature period throughout the measurement period. The total free radical species distribution is decrease from west to east in Lanzhou, which closely related to the distribution of the air pollutants. The total free radical oxidation capacity in polluted air roughly matches the effects of tobacco smoke produced by the incomplete combustion of a controlled amount of tobacco in a smoke chamber. A relatively unsophisticated chromatographic fingerprint similarity is used for indicating preliminarily the effect of total free radicals in polluted air on human health.

1. Introduction

Total free radical species (TFRs) include hydroxyl radical, hydroperoxyl radical, alcoxyl radicals, derived transition state species,

* Corresponding authors.
E-mail addresses: wangguoying@lut.cn (G. Wang), yhzhang@pku.edu.cn (Y. Zhang), shigaofeng@lut.cn (G. Shi).

http://dx.doi.org/10.1016/j.scitotenv.2017.07.233
0048-9697/

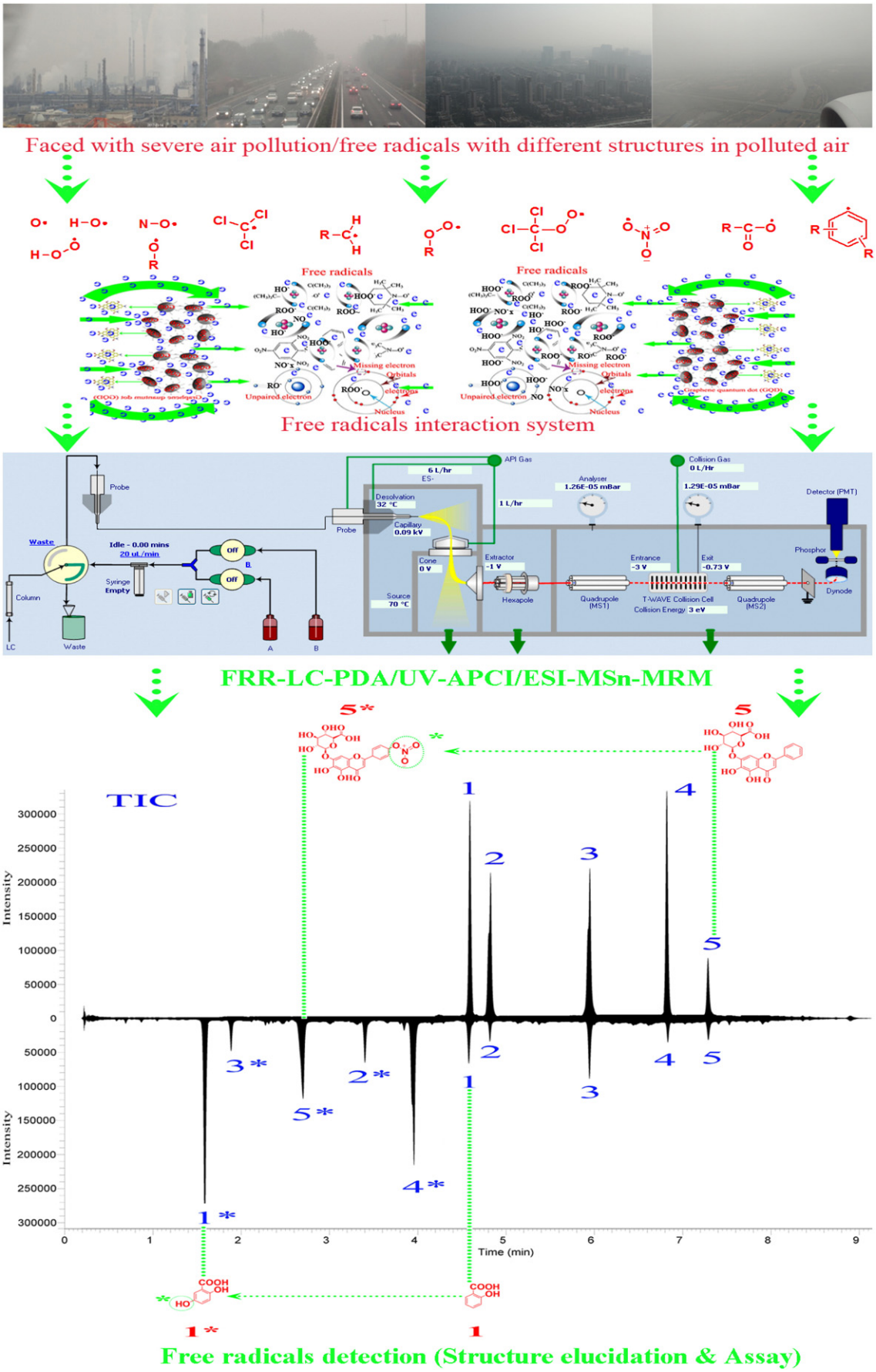

Scheme 1. Detection and evaluation of free radicals in polluted air based on FRR-LC-PDA/UV-APCI/ESI-MS^n-MRM.

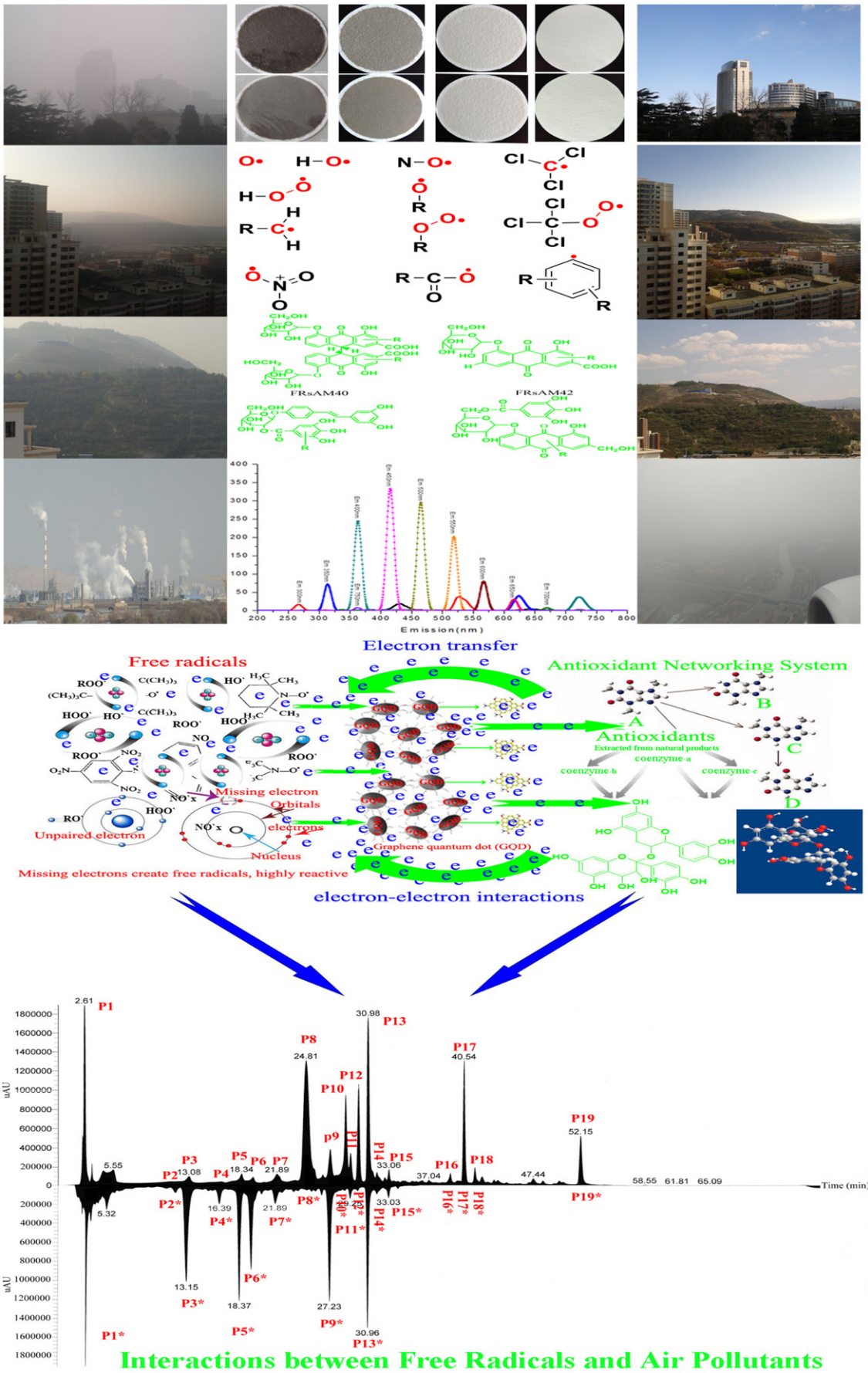

Scheme 2. Interaction mechanism between TFRs and fine particulate air pollution.

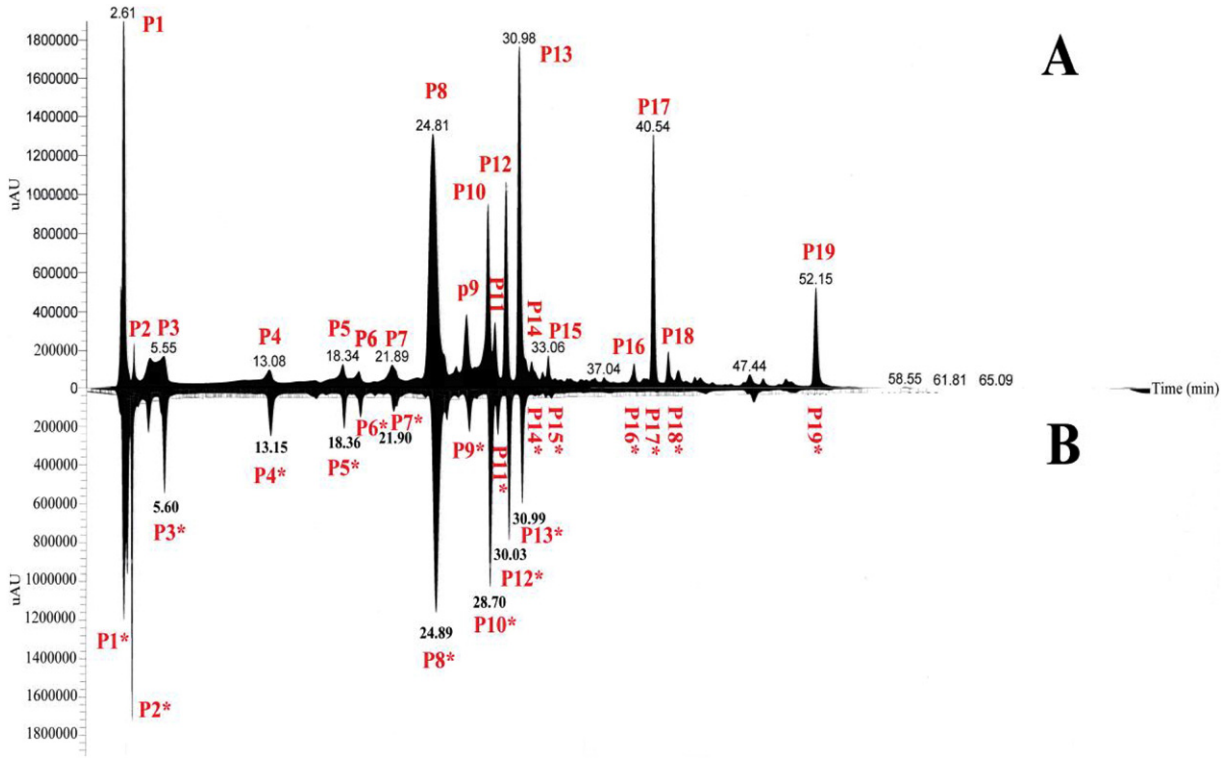

Fig. 1. FRR-LC-PDA/UV-APCI/ESI-MS^n-MRM chromatographic fingerprint of reactive molecules before and after reaction with TFRs in polluted air monitored at 360 nm: (A) before reaction with TFRs; (B) after reaction with TFRs in polluted air. (Distribution characteristics of free radicals in Lanzhou, general chromatographic fingerprint based on long-term detection).

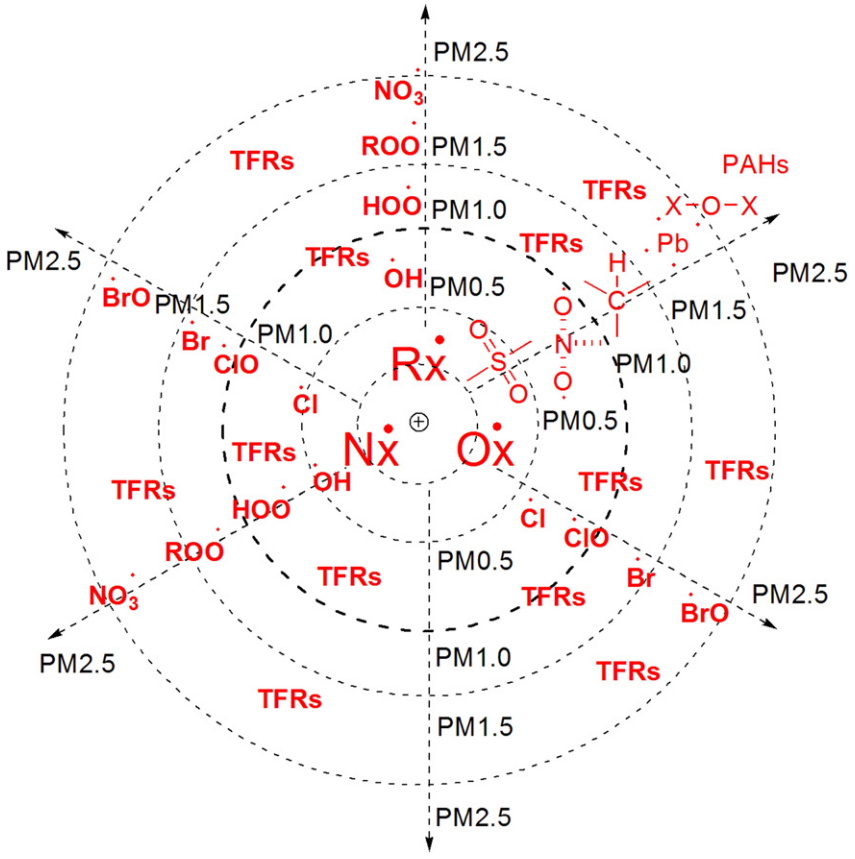

Scheme 3. Schematic diagram of correlation between TFRs and air pollutants.

intermediate species, and excited state species of chemical molecules. The role of TFRs in atmospheric chemistry was already recognized (Rohrer and Berresheim, 2006; Su et al., 2011; Chaudhuri et al., 2010; Zhang et al., 2008a; Chuang et al., 2016; Bartolomei and Wittmer, 2015; Eisele and Bradshaw, 1993; Wang et al., 2013, 2014; Lu et al., 2012; Li et al., 2014; Hofzumahaus et al., 2009; Welz et al., 2012; Dellinger and Pryor, 2000; Dellinger et al., 2001; Giuseppe, 2001; Cruz-Guilloty and Perez, 2011; Gligorovski and Weschler, 2013). The TFRs are colorless, odorless species and not easy to perceive by body, or even some instruments. The TFRs can react with air pollutants within about several seconds to 10^{-12} s. Scientists increasingly believe free radical plays a major role in the oxidizing power of the atmosphere and the development of aging-related diseases. Those TFRs also control the removal, transfer and secondary nucleation of nearly all gaseous atmospheric pollutants. A vast body of evidence has been presented in the last decade indicating that various man-made pollutants present significant risk to human health. Especially, more industry and automobile-based-petroleum-driven pollution are present in air. Smog is common in urban regions. Some health problems are forms of air pollution produced by the reaction of sunlight with gases (hydrocarbons, nitrogen, ozone) primarily released in factory and automobile exhaust. Various gases present in smog are oxidants and induce organ and cellular damage via generation of free radical species. As a large percentage of environmental pollutants undergo transformation (ex. oxidation, reduction) to convert into free radical species that induce various toxic insults (Bartolomei and Wittmer, 2015; Eisele and Bradshaw, 1993; Wang et al., 2013, 2014). The common theme with the wide range of air pollutes is the generation of free radicals (oxidative stress). Free radicals are commonly formed during oxidation processes. There is a considerable amount of free radicals in the air, especially contaminated environment. Whereas free radical interactions play an important role in the nucleation, formation, evolution, explosive growth, and dissipation of secondary fine particle pollutes. There is the fact that TFRs concentrations are influenced by thousands of air pollutants (Rohrer and Berresheim, 2006; Su et al., 2011; Chaudhuri et al., 2010; Zhang et al., 2008b). Moreover, owing to the short chemical lifetime, the TFRs concentrations are difficult to measure. The high variability of TFRs concentrations has prevented the detection of possible trends in the concentration of this species (Rohrer and Berresheim, 2006).

In this study, a novel method, by use of free radical reactions combined with liquid chromatography atmospheric pressure chemical & electrospray ionization and tandem mass spectrometry multiple reaction monitoring positive/negative ions analysis method (FRR-LC-PDA/UV-ESI/APCI-MS^n-MRM) to detect and identify the free radicals in polluted air (as illustrated in Scheme 1, schematic diagram), was developed. The method is useful and complementary extension for the detection of atmospheric free radicals in contaminated environment and for evaluating the effects of free radicals in polluted air on human health. Furthermore, the transferred or changed characterization of TFRs between polluting and non-polluting, and the interactions between TFRs and fine particulate air pollution (as illustrated in Schematic diagram 2) were investigated. The chemical structures and contents of TFRs were researched and the correlation between TFRs and air pollutants (ozone, particulate matters ex. PM 2.5, PM 10) was investigated (as illustrated in schematic diagram 3). The TFRs similarity between outdoor polluted air and tobacco generating smog and free radicals was evaluated and the fingerprint chromatographic similarity value was used for indicating the effects of total free radicals in polluted air on human health. All the out-filed experiments were carried out in Lanzhou area and more windless/inversion days (nearly 300 days per year, surface inversion about 200 days) persist in the year than other region. Lanzhou region has a less input and output of air pollutes from external region. Therefore, this region is an ideal natural laboratory for the research of free radicals in polluted air. The results in this region could provide reference data for the TFRs researches of other areas or large-scale regions.

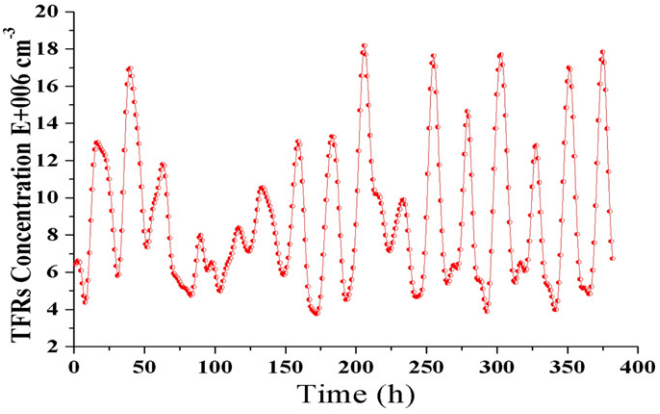

Fig. 2. The distributive characteristics of total free radicals in Lanzhou region for 24 h consecutive hours (August 20 to September 4, 2016).

2. Experimental

2.1. Reagents and materials

HPLC-grade acetonitrile (CH_3CN), HPLC-grade methanol (CH_3OH), HPLC-grade acetic acid (CH_3COOH), and HPLC-grade formic acid (HCOOH) were obtained from Merck (Darmstadt, Germany). Ultrapure water (H_2O, >18 MΩ) was prepared in laboratory. Natural graphite powder was obtained from Tianjin Guangfu Research Institute (Tianjin, China). The whole plant material Roxb. Ex Fleming H. Karst., Myricaria germanica, and azalea were obtained from the Tibetan hospital of Huangzhong of Qinghai province, China. The plant material Salvia miltiorrhiza, Willow bark (fresh), Scutellariae, natural gum, Olive leave, *Cistanche deserticola* and Licorice were collected from Qingyang, Tianshui, Longnan and Jiuquan Gansu province, China, respectively. LC-PDA/UV- ESI/APCI-MS^n-MRM mobile phases were prepared from HPLC-grade CH_3CN, CH_3OH, CH_3COOH, HCOOH, and H_2O. Unless otherwise stated, other reagents were of analytical grade and were used as received.

2.2. Preparation and purification of radical-scavenging natural reactive molecules

The whole plant materials were milled and extracted by maceration in ethanol/water (EtOH/H_2O), respectively; the plant extracts were

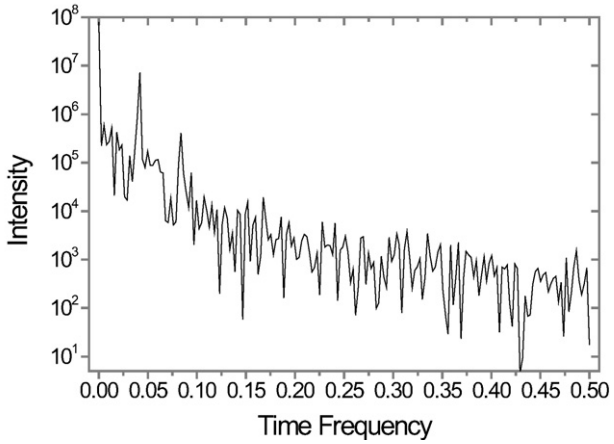

Fig. 3. The TFRs fluctuation range in a cycle period (Xigu District).

concentrated in a vacuum to syrup, diluted with ultrapure water and partitioned with n-Butanol, ethyl acetate (EtOAc), dichloromethane (CH_2Cl_2) and petroleum ether. Then, the n-Butanol-soluble portions layer, EtOAc-soluble portions layer, CH_2Cl_2-soluble portions layer and petroleum ether-soluble portions layer were evaporated in a vacuum to afford a residue. Each part was fist investigated for screening their free radical-scavenging capacities in vitro. The parts were subjected to column chromatography and reversed phase HPLC, respectively. Finally, purified compounds were obtained by repeated chromatography and recrystallized. The obtained compounds were used for the preparation of membrane by electrostatic spinning.

2.3. Preparation of electrostatic spinning membrane for trapping TFRs

3.0 mg purified compounds were weighed, then, added into 10 mL CH_3CH_2OH aqueous solution (80%), and labeled as Solution A, Solution B, Solution C, Solution D, Solution E, and Solution F respectively, and carried out the agitation and ultrasonic dissolving for 5 min at a temperature of 0 °C in circulating ethanol bath. Thus, the solutions were mixed and added in gum-ethanol solution, and agitated for 30 min. Then, the mixed solution (prepared spinning solution) was loaded into an electrospinning apparatus, and connected to a high-voltage supply. Then, the solution was fed using a pump at a rate of 1.6 mm/min. The distance between the solution spraying point and the collector was

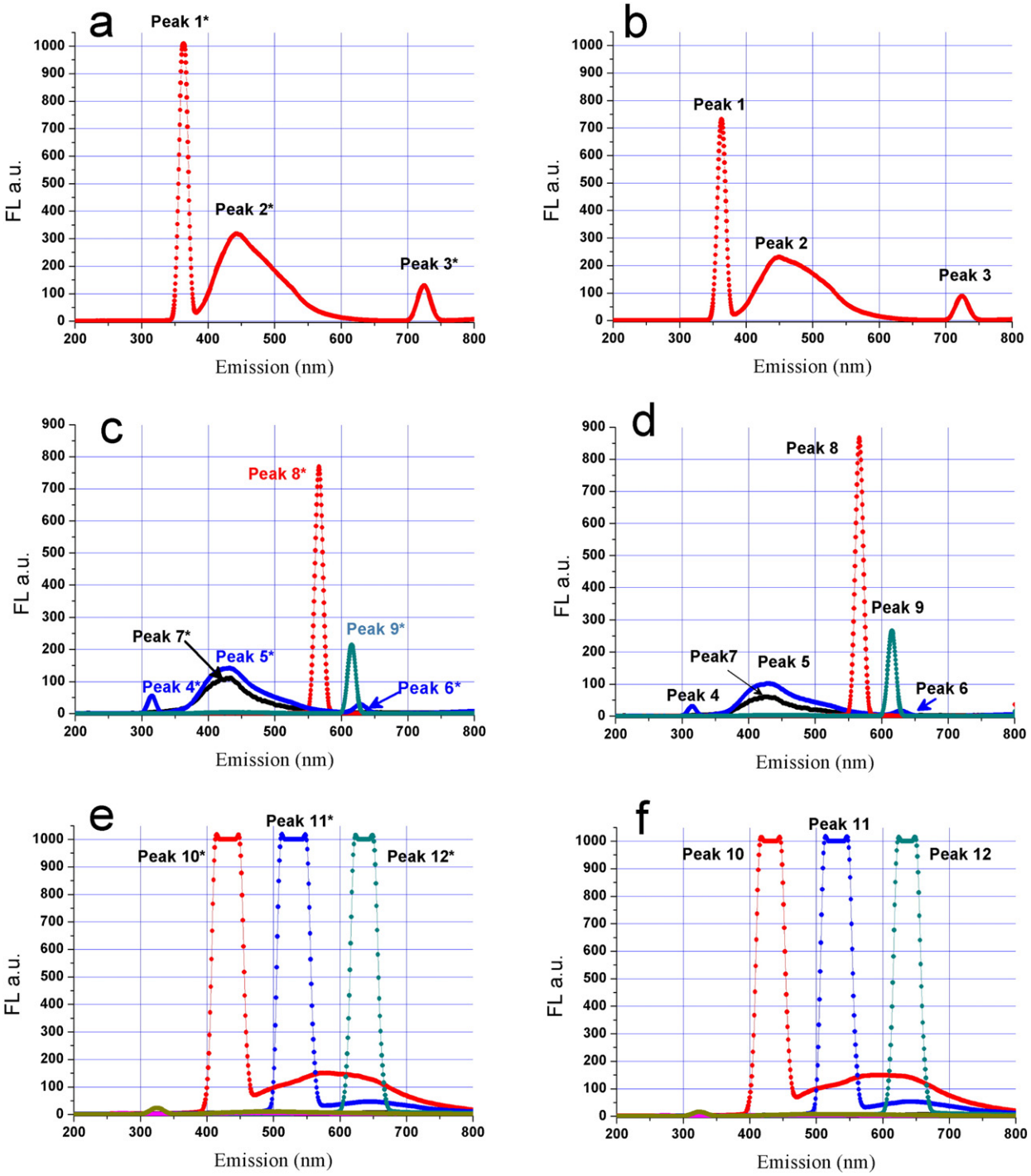

Fig. 4. The FL scan spectrum of TFRs reaction characteristics.

approximately 17 cm. A positive voltage of 12 kV, negative voltage of 3 kV was applied for electrostatic spinning. The optimal relative humidity and temperature was maintained 35% and 50 °C, respectively. At last, the electrostatic spinning membrane (ESM) for trapping TFRs was obtained.

2.4. Air sampling

A high-volume air sampling system was utilized for collecting the air samples. The above-prepared ESM was used for trapping TFRs in polluted air samples. The sampling flow rate was set at 100 L/min, and then carried out the reaction for 1 h under the natural ambient temperature. Thus, a free radical detecting ESM was obtained. The preparation of control sample ESM was the same as the above but without collecting the polluted air. After given time of sampling, the free radical detecting ESM and control sample ESM were dissolved into methanol/water solution, respectively. The reactive molecules solution was also used in TFRs scrubbing experiment (flow rate 0.8 L/min, reaction time 1–2 h). Then, the solutions were passed through 0.45 μm filter and injected for HPLC-PDA/UV-ESI/APCI-MS^n-MRM analysis, respectively. The changes in reactive molecules were measured by reading the peak areas of HPLC-PDA/UV and/or the intensities of HPLC-ESI/APCI-MS^n- MRM (as illustrated in Scheme 1 and Scheme 2).

2.5. Sampling sites

Four sampling sites were used from the west to the east in Lanzhou region. At the sampling sites, the sampler was placed outside building,

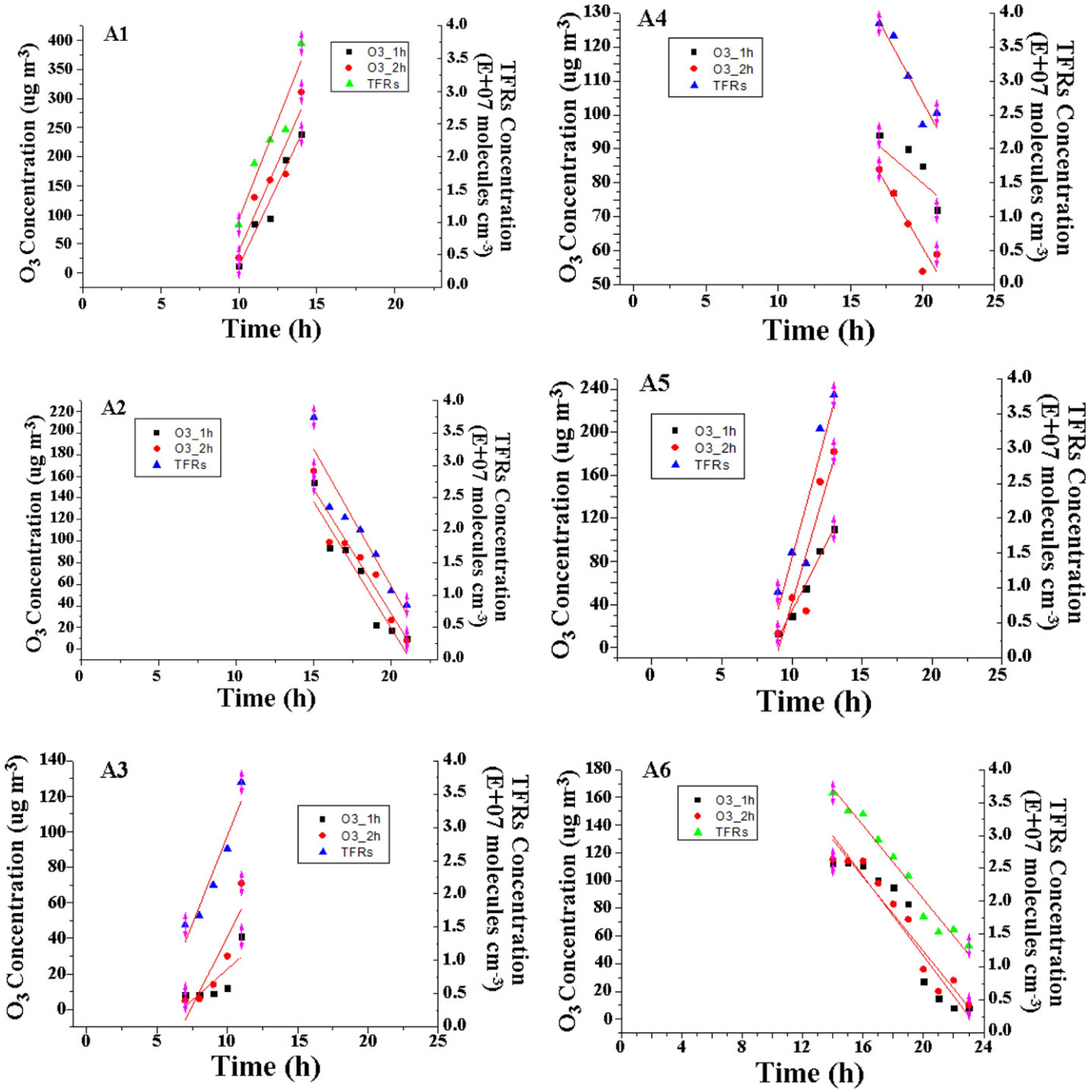

Fig. 5. Correlation of TFRs and ozone.

about 30 m from major traffic lane or major building. Four periods were monitored every day, 1 h each time. The sampling flow was calibrated regularly.

2.6. HPLC-PDA/UV-ESI/APCI-MS/MS analysis for detecting and identifying TFRs

HPLC-PDA/UV-ESI/APCI-MS/MS separations were done on a C_{18} column (3.0 μm, 150 × 2.1 mm i.d.) (Thermo Electron Corporation, USA) with a PDA/UV assay detection system. The separation conditions are as follow: flow rate 0.20 mL min^{-1}; separation temperature 40 °C; sample manager temperature 4 °C; PDA/UV wavelength from 190 nm to 800 nm; acquiring sample mode: partial loop with needle overfill; solvent A, 2.0% acetic acid and 8.0% methanol in water; solvent B, acetonitrile; starting from 3% to 10% B in 10 min, from 10% to 25% B in 30 min, from 25% to 45% B in 50 min, from 45% to 60% in 60 min, and keeping constant for 2 min; then from 60% to 70% B in 65 min, from 70% to 80% B in 70 min, from 80% to 100% B in 75 min, then from 100% to 3% B in 1 min and keeping constant for 15 min for reconditioning the HPLC-PDA/UV-ESI/APCI-MS/MS-MRM system.

The detection and identification of TFRs were done on an Ion Trap tandem mass system equipped with a multi-mode ESI/APCI ion source operating in both positive ion mode and negative mode. The tandem mass conditions were set as follow: ion mode: negative mode-APCI/ESI; Discharge Voltage: 3.5 kV; Capillary Temp: 145 °C; Vaporizer Temp: 380 °C; desolvation gas flow: 65 arb; cone gas flow: 20 arb; collision energy: 30–70 V; desolvation gas: nitrogen (99.999%); cone gas: nitrogen (99.999%); collision gas: argon (99.999%); Cappilary Voltage (v) −7; Tube Lens Offset (v) 6; Isolation width (*m*/*z*) 3; Normalized collision Energy(%) 50; Activation Q 0.30; Activation Time (msec) 50–500; Mutipole 1 Offset (v) 5; Lens Voltage (v) 5; Mutipole 2 Offset (v) 2; Mutipole RF Amplitude (v p-p) 0, Entrance Lens (v) 6; Full MS Target: 1e + 005; SIM Target: 1e + 006; MSn Target: 1e + 006; Ion Gauge Pressure: not higher than 1.50 × 10 e^{-5} Torr. The precision of mass determination drops in values of 10 to 550 ppm when using tandem mass Select ion monitoring Scan and Daughter Scan functions. All the control samples, experimental samples and reaction solutions must be passed through 0.22 μm filter in advance and then 2–100 μl of these were used for HPLC-PDA/UV-ESI/APCI- MS/MS-MRM analysis, respectively.

3. Results and discussion

3.1. Free radical signals amplification and detection in polluted air

A major pathway for production of TFRs is the interactions between ozone, volatile organic compounds and solar. Once TFRs formed, the TFRs react with tropospheric trace constituents within about several seconds or fewer seconds. Owing to the short chemical lifespan, the TFRs structures and concentrations are difficult to measure. The rapid reactions between free radicals in polluted air and reactive molecules resulted in the changes of molecular structure and/or molecular substance content. During the reactions between free radicals and reactive molecules, the electron transfers from the reactive molecules to the free radicals occurred, in the mean time, the molecular structures involved in the reactions would be decomposed or formed adducts and the molecular content involved in the reaction decrease. Newly experiment results are exciting, that is the reaction signals between the free radicals in polluted air and the reactive molecules can be amplified significantly. Furthermore, the reaction signals can be effectively captured and reflected accurately and intuitively by FRR-LC-PDA/UV-APCI/ESI-MS^n-MRM in polluted air (Fig. 1).

The TFRs fingerprint of Lanzhou was obtained, which indicated the common features and the characteristics of TFRs in polluted air in this area. The integrating peak area of the reactive molecular would decrease or disappear in the LC-PDA/UV chromatogram and/or APCI/ESI-MS^n-MRM profile after the interaction with the free radicals in polluted air (Fig. 1 A and B, Peak 1 & 1*, 9 & 9*, 12 & 12*, 13 & 13*, 14 & 14*, 15 & 15*, 16 & 16*, 17 & 17*, 18 & 18*, and 19 & 19*.). Moreover, some integrating peak area of the reactive molecular forming adducts between TFRs and molecules interaction would increase or emerging new peaks (Fig. 1 A and B, Peak 2 & 2*, 3 & 3*, 4 & 4*, 5 & 5*, 6 & 6*). While for the air without free radicals in it, there was almost no change in the integrating peak area, such as Fig. 1 A and B, Peak 7 & 7*, 8 & 8*, 10 & 10*, and 11 & 11*. The changes in chromatographic peak areas and retention times are used to quantify the TFRs concentration and identify the structures. Many free radical reactive molecules have been screened and the reactive sites (functional groups in molecule) have been stored in free radical reactive molecules database. The free radical reaction signals before and after experiment can be effectively captured and visually read by FRR-LC-PDA/UV-APCI/ESI-MS^n-MRM in polluted air. All the free radical information (rapid determination of free radicals and identification of it structure) in polluted air can be presented in an easy-to-read chromatographic fingerprint.

Table 1
Linear fitting results of TFRs and ozone.

Equation	y = a + b * x	Value	Standard error
(A1)			
Adj. R-square	0.9422	0.8549	0.8883
O3_1h	Intercept	−553.40	83.91
O3_1h	Slope	56.50	6.94
O3_2h	Intercept	−572.60	148.72
O3_2h	Slope	61.00	12.31
TFRs	Intercept	−591.34	144.07
TFRs	Slope	68.31	11.92
(A2)			
Adj. R-square	0.9026	0.9083	0.8845
O3_1h	Intercept	487.71	56.38
O3_1h	Slope	−23.43	3.11
O3_2h	Intercept	492.71	53.58
O3_2h	Slope	−23.00	2.95
TFRs	Intercept	565.64	67.09
TFRs	Slope	−25.38	3.70
(A3)			
Adj. R-square	0.4661	0.7401	0.8952
O3_1h	Intercept	−47.40	30.08
O3_1h	Slope	7.00	3.30
O3_2h	Intercept	−115.20	40.37
O3_2h	Slope	15.60	4.43
TFRs	Intercept	−101.23	30.53
TFRs	Slope	19.88	3.35
(A4)			
Adj. R-square	0.1915	0.8254	0.8462
O3_1h	Intercept	152.00	49.14
O3_1h	Slope	−3.60	2.57
O3_2h	Intercept	207.10	31.17
O3_2h	Slope	−7.30	1.63
TFRs	Intercept	261.24	31.23
TFRs	Slope	−7.86	1.63
(A5)			
Adj. R-square	0.9816	0.7965	0.8146
O3_1h	Intercept	−221.10	19.28
O3_1h	Slope	25.50	1.73
O3_2h	Intercept	−404.80	121.17
O3_2h	Slope	44.60	10.92
TFRs	Intercept	−397.68	123.73
TFRs	Slope	48.08	11.15
(A6)			
Adj. R-square	0.8683	0.9283	0.9666
O3_1h	Intercept	334.27	34.78
O3_1h	Slope	−14.43	1.85
O3_2h	Intercept	317.23	23.16
O3_2h	Slope	−13.41	1.23
TFRs	Intercept	352.56	15.38
TFRs	Slope	−13.30	0.82

The changes in chromatographic peak areas (integral peak areas) are used to quantify the free radicals' concentration. Moreover, the extracted ion chromatograms of the changed ions could provide additional information regarding the molecular structure of TFRs. For this reason, the FRR-LC-PDA/UV-APCI/ESI-MS/MS method provides absolute advantage in the structure elucidation of free radicals in polluted air. Because FRR-LC-PDA/UV coupled with a tandem mass detector is an ideal tool for characterizing free radical's structures (Schemes 1, 2 and 3), it is practicable to identify those free radicals in polluted air that are not easy measurable due to their high reactivity and very short half-life (10^{-12} s to several seconds). The structure analysis of free radicals can be compared the intensities of individual ion peaks in negative and/or positive ion models between the control and polluted air samples. Reactive molecules (reflect in integral area of ion peaks) that reacted with TFRs showed decrease intensities or the reactive molecular peaks disappeared. For example, these changed potential peaks included the components with mass charge ratio (m/z) of molecules. Tandem mass was used to elucidate the molecular structures of different corresponding TFRs. Based on the control experiments and total ion current (TIC) of the TFRs samples, the TFRs adducts molecular mass could be gained in the total ion current in positive or negative ion modes. To confirm the TFRs structures, MS^2, MS^3 and MS^n of those ion peaks were further investigated.

3.2. TFRs distribution and obvious correlative factors in polluted air

The total free radicals in polluted air in Lanzhou region were detected by the developed FRR-LC-PDA-APCI/ESI-MS/MS-MRM. The concentration values of the total free radicals were determined for consecutive years. In Lanzhou region, there are a number of distinguishing characteristics with relatively little input and output of atmospheric pollutants, therefore, those areas could be regarded as a natural laboratory for the TFRs outfield experimental research. The distributive characteristics of total free radicals show obvious features of the wave-type. The results are shown in Fig. 2.

There are significant "peaks" and "valleys" characteristics. Moreover, the TFRs concentration values showed an upward trend overall slowly in recent years. The TFRs distributive concentration changed from strong to weak from west (Xigu District) to east (Donggang District). Based on the overall data analysis in Lanzhou region, the TFRs concentration showed 'simple harmonic vibration' characteristics (Fig. 3) in every cycle period, which is similar to the attenuation of vibration. The result shows that the TFRs are varying at a period of waves. The TFRs concentration in this region varied from 7.80E + 07 to 0.45E + 01 and then entered the next cycles.

From the simultaneous pollutant monitoring data, we also found that the TFRs concentration values related with contaminated matters. The total free radicals correlated with the oxidizing levels of the polluted air in the region. Moreover, the NO_2, SO_2, O_3, CO, and especially fine particulate matters play an important detrimental feedback role on the TFRs. Perhaps more significant, the TFRs concentration values associated with the fluorescence response signals in the polluted air. We find that the TFRs concentration values can be described by a linear dependence on the fluorescence response signals throughout the measurement period. However, the fluorescence response signals affected the visibility, where the fluorescence response signals increased, the visibility at the Lanzhou City's came down to low levels. At relatively low temperature conditions, the fluorescence response signals (fluorescent components) increase with the increase of particulate matters. However, at relatively high temperature conditions, the fluorescence response signals (fluorescent components) change with the change of ozone.

In the relevant correlation, one of the most important characteristic of TFRs distribution is that the particulate matters are "booming" at some certain periods related with TFRs variation. The TFRs peak value and particulate matters "booming" period appeared generally in low-temperature (around or less than minus three degrees Celsius) period. The particulate matters "booming" period could be delayed about 2–5 h after the TFRs peak value appeared (without significant weather variation conditions). Moreover, in the tracking experiments, we also found that the newly formed particles would initiate second TFRs peak values. By analyzing the causes of TFRs and particles interaction, the fluorescence (FL) spectrum results (Fig. 4a–f) reveal that the excited transition of particulate matters can facilitate TFRs formation in polluted air, and the newly emerging TFRs could promote the growth of fine particulate matter. The researches show that the TFRs distribution is closely related to the fine particulate matter growth under low-temperature period, but the correlation time is delayed about 2–5 h.

The general chart of TFRs FL scan spectrum from 250 nm–750 nm (Fig. 4a–f) show the full range of TFRs reaction characteristics. From 300 nm to 650 nm, there are significant FL intensity. The FL intensity increased from peak 1 (the results are shown in Fig. 4a and b) 730.96 a.u., 363.0 nm to peak 1* 1008.64 a.u. (increase), 363.5 nm (red shifts), from peak 2231.02 a.u., 449.5 nm to peak 2* 317.97 a.u. (increase), 442.5 nm (blue shifts), from peak 3 89.15 a.u., 725 nm to peak 3* 129.82 a.u. (increase), 725.0 nm (no change). The FL intensity changed from peak 4 (the results are shown in Fig. 4c and d) 30.98 a.u., 315.50 nm to peak 4* 55.39 a.u. (increase), 315.0 nm (blue shifts), from peak 5101.95 a.u., 430.0 nm to peak 5* 141.72 a.u. (increase), 431.5 nm (red shifts), from peak 6 16.14 a.u., 628.5 nm to peak 6* 28.01 a.u. (increase), 628.5 nm (no change), from peak 7 60.61 a.u., 424.0 nm to

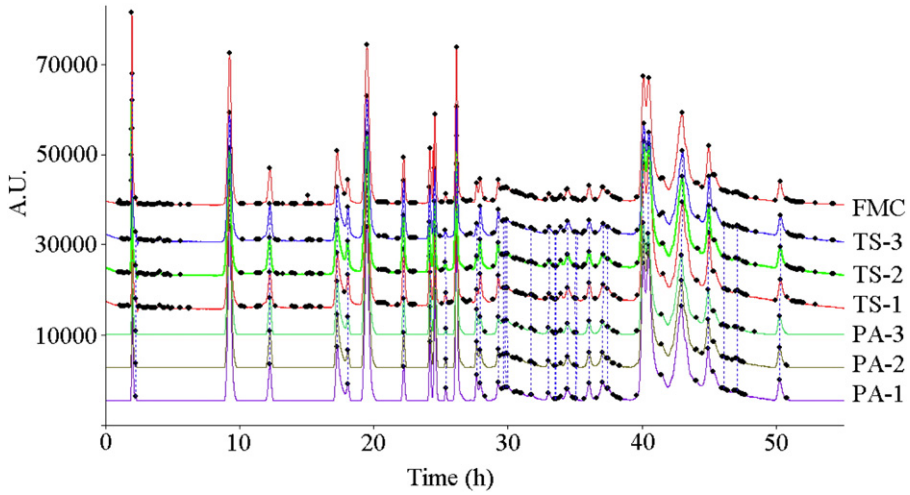

Fig. 6. The TFRs similarity between outdoor polluted air and tobacco smoke.

Table 2
The similarity data of TFRs in outdoor polluted air and tobacco smoke.

	PA-1	PA-2	PA-3	TS-1	TS-2	TS-3	FMC
PA-1	1.000	0.989	0.983	0.966	0.970	0.963	0.991
PA-2	0.989	1.000	0.988	0.971	0.970	0.970	0.993
PA-3	0.983	0.988	1.000	0.940	0.961	0.968	0.985
TS-1	0.966	0.971	0.940	1.000	0.979	0.966	0.982
TS-2	0.970	0.970	0.961	0.979	1.000	0.993	0.990
TS-3	0.963	0.970	0.968	0.966	0.993	1.000	0.988
FMC	0.991	0.993	0.985	0.982	0.990	0.988	1.000

Note: Retention time (RT), Fingerprint mutual characteristic (FMC), Tobacco Smoke (TS), Polluted Air (PA).

peak 7* 108.72 a.u. (increase), 419.0 nm (blue shifts). However, the FL intensity changed from peak 8 (the results are shown in Fig. 4c and d) 866.99 a.u., 566.5 nm to peak 8* 768.89 a.u. (decrease), 566.5 nm (no change), from peak 9266.29 a.u., 615.5 nm to peak 9* 213.94 a.u. (decrease), 615.5 nm (no change). Fig. 4e and f show that there is almost no change in the FL intensity of peak 10, peak 10*, peak 11, peak 11*, peak 12 and peak 12*. If the air temperature over a large area remain at or below minus three degrees centigrade, the particulate matter peak value appeared after the increased FL intensity of TFRs peak value at short wavelength (with higher energy), such as 363.5 nm, 442.5 nm, 315.0 nm, 431.5 nm and 419.0 nm. During the tracking and monitoring process, there are significant aggregation trend to the fine particulate matter under the above conditions. More free radicals could produce in polluted air when the temperature remain at or below minus three degrees.

However, another important aspect of TFRs based on long-term detection of TFRs in Lanzhou region, we find that the concentration value of the TFRs can be described by a linear delay dependence on ozone throughout the detection period, when the temperature could stay above zero in daytime or warmer times of year. The results and regression equation are shown in Fig. 5A1–A6 and Table 1A1–A6. The investigation shows there are positive increase-correlation (Fig. 5A1, A3, and A5) and positive decrease-correlation (Fig. 5A2, A4, and A6) between TFRs and ozone, despite the fact that the TFRs and ozone concentration values are affected by numerous reactants.

3.3. The effects of TFRs in polluted air on human health

In polluted air, there is a considerable amount of TFRs, which can easily be inhaled from outdoor and indoor polluted air, then causing free radical chain reactions during oxidation processes occurring in living organisms. The TFRs, known to be responsible for health damage and accelerated aging, play a major role in the development of aging-related diseases (including inflammatory disorder, cardiovascular diseases, arthritis, Parkinson's, Alzheimer's, premature aging, and cancer). In tissues, free radicals can damage cells and are believed to accelerate the progression of cancer and cardiovascular disease.

The TFRs are a kind of contaminants with colorless, tasteless characteristics, and almost imperceptible by human body, however, the unpaired electrons characteristics make the TFRs highly chemically reactive towards air pollutants and/or tissues, or even towards themselves. Because of the difficulties to the measurement of TFRs, the TFRs have not been included in the environmental monitoring indicators. The TFRs transferred with secondary pollutants, and closely related with fine particulate matters and ozone. The earlier experiments showed that the TFRs determine the oxidizing power of the atmosphere in some local areas. In our study, the concentration of TFRs in polluted air was determined and calculated as the equivalent pollution index of tobacco smoke, that is, the TFRs concentrations and oxidizing power in polluted air were compared to the content of free radicals in tobacco smoke (produced by the incomplete combustion of a controlled amount of tobacco in a smoke chamber).

Table 3
The correlation data of TFRs in outdoor polluted air and tobacco smoke.

RT (min)	PA-1	PA-2	PA-3	TS-1	TS-2	TS-3	FMC	RT RSD (%)	PA &TS RSD (%)	Matching number
2.12	226,923	215,395	204,719	210,377	204,657	197,699	209,962	0.13	4.87	6
2.45	3500	2984	2403	18,240	18,387	17,763	10,546	0.11	78.87	6
10.05	672,586	683,026	692,860	536,046	543,663	550,450	613,105	0.04	12.52	6
13.31	108,086	110,142	111,056	148,119	152,192	152,411	130,334	0.04	17.35	6
18.76	240,260	237,164	234,074	284,404	287,660	281,884	260,908	0.02	10.02	6
19.64	47,443	47,692	46,784	104,323	105,559	110,233	77,006	0.04	42.33	6
21.17	797,213	824,271	848,909	650,488	672,410	692,374	747,611	0.02	11.47	6
24.16	78,905	80,661	82,760	162,448	165,393	169,769	123,323	0.01	37.85	6
26.27	110,048	112,958	116,476	101,207	103,816	107,659	108,694	0.05	5.23	6
26.68	225,254	223,555	222,092	158,949	154,804	155,169	189,970	0.04	19.43	6
27.56	20,139	12,722	6715	25,737	16,810	12,779	15,817	0.04	41.91	6
28.43	415,223	395,735	379,987	334,911	321,532	311,035	359,737	0.01	11.95	6
30.06	55,527	51,677	51,754	26,530	25,720	25,449	39,443	0.02	37.79	6
30.36	54,733	57,989	53,003	88,576	89,475	91,138	72,486	0.03	26.18	6
31.82	48,619	45,762	49,117	78,654	76,910	73,312	62,062	0.01	25.34	6
32.22	11,397	32,255	39,855	30,242	9605	8989	22,057	0.03	61.74	6
32.40	7096	13,619	9755	8544	5637	7630	8713	0.03	31.82	6
32.54	48,412	39,903	73,198	10,258	11,475	56,105	39,892	0.06	62.72	6
34.46	1737	1055	2952	3670	3253	2896	2594	0.02	38.22	6
35.92	24,377	21,859	19,195	20,400	23,088	22,123	21,840	0.04	8.48	6
36.42	318	285	266	352	498	285	334	0.03	25.72	6
36.48	941	509	140	430	530	494	507	0.02	50.61	6
37.44	29,458	48,750	46,231	63,902	64,895	61,924	52,527	0.06	26.34	6
38.10	1094	1260	574	2422	1623	2280	1542	0.05	46.24	6
38.17	1368	758	453	2185	2464	856	1347	0.1	60.64	6
39.19	56,865	48,956	43,147	66,754	58,844	51,124	54,282	0.04	15.31	6
40.29	89,110	65,811	59,923	94,100	72,851	30,436	68,705	0.02	33.37	6
40.69	7329	6940	4744	40,744	5090	5210	11,676	0.02	122.30	6
43.59	534,045	486,685	463,493	564,849	518,574	470,723	506,395	0.05	7.82	6
44.01	829,085	700,566	558,615	859,612	722,131	576,422	707,738	0.07	17.59	6
46.72	766,652	711,572	659,254	804,140	750,190	690,146	730,326	0.09	7.29	6
48.87	163,191	154,027	155,511	210,361	201,245	192,355	179,448	0.09	13.83	6
50.13	1379	2866	2794	1403	1975	1042	1910	0.01	40.49	6

Note: Retention time (RT), Fingerprint mutual characteristic (FMC), Tobacco Smoke (TS), Polluted Air (PA); the data based on optimal matching number.

In the course of the research, fifteen grams of the tobacco powder were added in a combustion cell, and then kindled the tobacco in a smoke chamber (Volume: 455 cm * 435 cm * 265 cm). The reactive molecule solutions were added into an automatic sequential air sampler. After sampling for 1–8 h from outdoor polluted air and smoke chamber, the samples were collected for evaluating the oxidation capacity by FRR-LC-PDA/UV-APCI/ESI-MS/MS-MRM, respectively. Based on the research data from Lanzhou region, we found that the TFRs similarity (oxidation equivalent) between outdoor polluted air and fifteen grams tobacco was higher than 0.982, the maximum reach 0.993. The matching degree of 33 peaks reached 6. The retention time RSD is <0.13%. The RSD of integral area of peaks varied from 5 to 40%. Those changes illustrated the high variability and high activity of TFRs. The results are shown in Fig. 6, Table 2, and Table 3. The similar results could indicate indirectly the effects of TFRs in polluted air on human health. The oxidation equivalent evaluation is only rough comparison by similarity (Liquid chromatography atmospheric pressure chemical & electrospray ionization and tandem mass spectrometry multiple reaction monitoring positive/negative ions analysis method). Because of previous environmental toxicology researches, the health risk data of tobacco smoke and environmental tobacco smoke (secondhand smoke) have become known. However, in general the related data on the further evidence of total free radicals in polluted air on the health risk are still scarce and lacks consistency. The preliminary results in this paper may provide a reference to study further the health risk of total free radicals in polluted air. More work will be needed to confirm the result because the study was based on a small, distinctive environmental condition.

4. Conclusions

The total free radicals have a very short half-life (approximately several seconds to 10^{-12} s), however, it plays a major role in the oxidizing capacity of the atmosphere in polluted air and the development of aging-related diseases in living organisms. The total free radicals also control the removal, transfer and secondary nucleation of nearly all gaseous atmospheric pollutants. Various gases present in haze are oxidants and induce organ and cellular damage via generation of free radical species. As a large percentage of environmental pollutants undergo oxidation or reduction of transformation to convert into free radical species that induce various toxic insults. Here we present and analyze measurements of atmospheric TFRs concentration in long-term period. The TFRs distributing characteristics in polluted air have been effectively captured and reflected accurately and intuitively by FRR-LC-PDA/UV-APCI/ESI-MS^n-MRM. The TFRs distribution is closely related to the fine particulate matter growth under low-temperature period, but the correlation time is delayed about 2–5 h. When the temperature could stay above zero during the warmer times of year, we find that the TFRs concentration value can be described by a linear delay dependence on ozone throughout the detection period. The distributive concentrations of total free radicals and air pollutants ($PM_{2.5\ \&\ 10}$, NO_2, SO_2, CO and O_3) in Lanzhou changed from strong to weak from west (Xigu District) to east (Donggang District). The TFRs concentration in polluted air roughly matches the effects of tobacco smoke (produced by the incomplete combustion of a controlled amount of tobacco in a smoke chamber) on human health. The similar results could indicate indirectly the effects of TFRs in polluted air on human health. The atmospheric free radicals researches provided the underlying basis for better understanding the atmospheric oxidizing capacity, fine particulate matter, and ozone formation and supporting the development of health prevention against air pollution and the execution of emission control strategy.

Acknowledgements

This work was supported by the National Key Research and Development Program of China [grant number 2016YFC0202900]; the National Natural Science Foundation of China [grant numbers 21407072, 21567015]; the Longyuan Youth Innovative Support Program of Gansu Province [grant number 2014]; and the Hongliu Natural Science Foundation of Lanzhou University of Technology [grant number 201403].

Appendix A. Supplementary data

Supplementary data to this article can be found online at http://dx.doi.org/10.1016/j.scitotenv.2017.07.233.

References

Bartolomei, E.G.A., Wittmer, J., 2015. Combustion processes as a source of high levels of indoor hydroxyl radicals through the photolysis of nitrous acid. Environ. Sci. Technol. 49 (11), 6599–6607.
Chaudhuri, L., Sarsour, E.H., Goswami, P.C., 2010. 2-(4-Chlorophenyl)benzo-1,4-quinone induced ROS-signaling inhibits proliferation in human non-malignant prostate epithelial cells. Environ. Int. 36 (8), 924–930.
Chuang, G.C., Xia, H., Mahne, S., Varner, K.J., 2017. Environmentally Persistent Free Radicals Cause Apoptosis in HL-1 Cardiomyocytes. Cardiovasc. Toxicol. 17 (2), 140–149.
Cruz-Guilloty, F., Perez, V.L., 2011. Molecular medicine: defence against oxidative damage. Nature 478 (7367), 42–43.
Dellinger, B., Pryor, W.A., Cueto, R., 2001. Role of Ircc radicals in the toxicity of airborne fine particulate matter. Chem. Res. Toxicol. 14 (10), 1371–1377.
Dellinger, B., Pryor, W.A., 2000. The role of combustion-generated radicals in the toxicity of PM 2.5. Proc. Combust. Inst. 28 (2), 2675–2681.
Eisele, F.L., Bradshaw, J.D., 1993. The elusive hydroxyl radical. Measuring OH in the atmosphere. Anal. Chem. 65 (21), 927A–938A.
Giuseppe, R.C., 2001. Quinoid redox cycling as a mechanism for sustained free radical generation by inhaled airborne particulate matter. Free Radic. Biol. Med. 31 (9), 1132–1138.
Gligorovski, S., Weschler, C.J., 2013. The oxidative capacity of indoor atmospheres. Environ. Sci. Technol. 47 (24), 13905–13906.
Hofzumahaus, A., Rohrer, F., Lu, K., Bohn, B., Brauers, T., Chang, C.C., Fuchs, H., Holland, F., Kita, K., Kondo, Y., Li, X., Lou, S.R., Shao, M., Zeng, L.M., Wahner, A., Zhang, Y.H., 2009. Amplified trace gas removal in the troposphere. Science 324 (5035), 1702–1704.
Li, X.Q., Lu, K.D., Wei, Y.J., Tang, X.Y., 2014. Technique Progress and Chemical Mechanism Research of Tropospheric Peroxy Radical in Field Measurement. 26 (4), 682–694.
Lu, K.D., Rohrer, F., Holland, F., et al., 2012. Observation and modelling of OH and HO 2 concentrations in the Pearl River Delta 2006: a missing OH source in a VOC rich atmosphere. Atmos. Chem. Phys. 12 (3), 1541–1569.
Rohrer, F., Berresheim, H., 2006. Strong correlation between levels of tropospheric hydroxyl radicals and solar ultraviolet radiation. Nature 442 (7099), 184–187.
Su, H., Cheng, Y., Oswald, R., Behrendt, T., Trebs, T., Meixner, F.X., Andreae, M.O., Cheng, P., Zhang, Y.H., Poschl, U., 2011. Soil nitrite as a source of atmospheric HONO and OH radicals. Science 333 (6049), 1616–1618.
Wang, G., Shi, G., Chen, X., 2013. Loading of free radicals on the functional graphene combined with liquid chromatography-tandem mass spectrometry screening method for the detection of radical-scavenging natural antioxidants. Anal. Chim. Acta 802, 103–112.
Wang, G., Niu, X., Shi, G., et al., 2014. Functionalized graphene quantum dots loaded with free radicals combined with liquid chromatography and tandem mass spectrometry to screen radical scavenging natural antioxidants from Licorice and Scutellariae. J. Sep. Sci. 37 (24), 3641–3648.
Welz, O., Savee, J.D., Osborn, D.L., Vasu, S.S., Percival, C.J., Shallcross, D.E., Taatjes, C.A., 2012. Direct kinetic measurements of Criegee intermediate (CH2OO) formed by reaction of CH2I with O2. Science 335 (6065), 204–206.
Zhang, Y.H., Hu, M., Zhong, L.J., 2008a. Regional integrated experiments on air quality over Pearl River Delta 2004 (PRIDE-PRD2004): overview. Atmos. Environ. 42 (25), 6157–6173.
Zhang, Y.H., Su, H., Zhong, L., 2008b. Regional ozone pollution and observation-based approach for analyzing ozone–precursor relationship during the PRIDE-PRD2004 campaign. Atmos. Environ. 42 (25), 6203–6218.